ISOSPIN IN MESON–MESON RESONANCES DERIVED IN THE 'T HOOFT MODEL

Z. Batiz, M.T. Peña

Centro de Física Teórica de Partículas, Instituto Superior Técnico
Av. Rovisco Pais 1049-001, Lisboa, Portugal

A. Stadler

Centro de Física Nuclear da Universidade de Lisboa
Av. Gama Pinto 2, 1649-003 Lisboa, Portugal
and
Departamento de Física, Universidade de Évora
Colégio Luís Verney, 7000-671 Évora, Portugal

(Received June 22, 2006; revised version received October 3, 2006)

Meson–meson scattering amplitudes within the 't Hooft model are considered. The results show that within this model the meson–meson scattering at low energies proceeds by the exchange of an isoscalar σ-like resonance, as well as of an isovector ρ-like resonance. Masses and widths for those resonances are calculated, and their dependence on the quark masses and the quark–gluon coupling strength is studied.

PACS numbers: 13.75.Lb, 13.75.–n, 12.38.–t

1. Introduction

In a previous article [1] we discussed pion–pion scattering within the 't Hooft model. We were able to obtain a σ-like resonance in the pion–pion scattering amplitudes. That calculation, however, did not consider isospin and gluon exchange. The motivation for correcting these two aspects was twofold: first, we expected to get more realistic masses and widths, and second, we wanted to check the findings of [2] using Minkowski space calculations. Although the values for the mass and width of the isoscalar (σ) resonance did change slightly in the desired direction, our model is still unphysical. However, the amplitudes observe the right chiral limit even without the gluon exchange contribution. This contradicts the conclusions of references [2] and [3], where a Euclidean metric was used, although the dimensionality was not truncated. It appears that the Euclidian metric is a more serious handicap than the truncated dimensionality.

2. Our model

We used the 't Hooft model description of microscopic QCD and assumed equal bare quark masses for both flavors as in the work of Cotanch and Maris [2]. The difference between Ref. [2] and our work lies in the fact that we use 1+1 dimensional Minkowski space instead of 4-dimensional Euclidean space. Our calculation maybe more rigorous, but the price that we pay for a reduced phenomenological content of our model is a lesser realistic description of the sigma and rho masses and widths.

2.1. Quark exchange diagrams

Here, as in our former work [1], we calculated the box and crossed box diagrams represented respectively in Fig. 1 and in Fig. 2. In Ref. [2] the authors considered also the quark exchange diagram represented in Fig. 3.

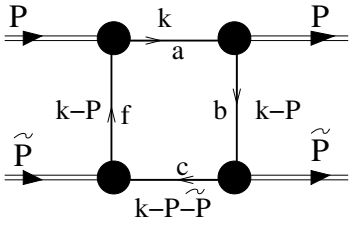

Fig. 1. The simplest box diagram. a, b, c and f denote the quark flavors.

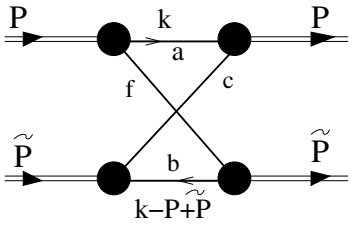

Fig. 2. Crossed box diagram.

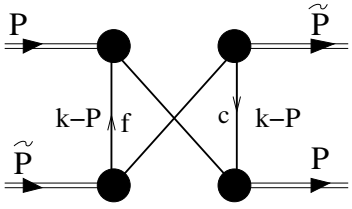

Fig. 3. The crossed box diagram we did not consider in [1].

In the present paper we follow them and also include it. It turns out that the contribution of the first and the third diagrams are proportional. We studied only the forward scattering case (as the authors of [2]) and computed the amplitudes $\mathcal{M}_I$ where the subscript I denotes the isospin $I = 0,\ 1,\ 2$ corresponding to the projections of the total amplitude on the three possible asymptotic isospin channels. Now let us discuss each box separately. First we recall the usual pion wave functions:

$$\begin{aligned} |\pi^+\rangle &= -|u\bar{d}\,\rangle\,, \\ |\pi^0\rangle &= \frac{1}{\sqrt{2}}|u\bar{u} - d\bar{d}\,\rangle\,, \\ |\pi^-\rangle &= |d\bar{u}\,\rangle\,, \end{aligned} \tag{1}$$

which we rewrite as:

$$\begin{aligned} |\pi^+\rangle &= -\delta_{au}\delta_{bd}\,\Psi_{ab}(k,P)\,, \\ |\pi^0\rangle &= \frac{1}{\sqrt{2}}(\delta_{au}\delta_{bu} - \delta_{ad}\delta_{bd})\,\Psi_{ab}(k,P)\,, \\ |\pi^-\rangle &= \delta_{ad}\delta_{bu}\,\Psi_{ab}(k,P)\,, \end{aligned} \tag{2}$$

where $\Psi_{ab}(k,P)$ is the wave function determined as in [1], as a function of the quark momentum k, the bound state momentum four-momentum P and the flavors a and b.

Given this quark structure, it is straightforward to determine the specific charge reactions to which each of the diagrams in Figs. 1–3 is linked. The direct box diagram B_1 (Fig. 1) contributes to two reactions, namely the $\pi^+\pi^0 \to \pi^+\pi^0$ and the $\pi^+\pi^- \to \pi^+\pi^-$ scattering reactions. In the first case, the intermediate quark flavors are $a = u$, $b = c = f = d$ or $a = \bar{d}$, $b = c = f = \bar{u}$. For the second reaction one has $a = c = u$, $f = b = d$ or $a = c = \bar{d}$, $f = b = \bar{u}$. Therefore the box diagram B_1 contributes twice for each of the reactions. The symmetrized diagram (in terms of the outgoing meson momenta) corresponds to backward scattering of these very same reactions, and therefore does not contribute to forward scattering.

The crossed box diagram B_2 (Fig. 2) also contributes to two different channels with two different possible quark flavor combinations possible for each. For the $\pi^+\pi^0 \to \pi^+\pi^0$ scattering reaction either $a = u$, $b = c = f = d$ or $a = \bar{d}$, $b = c = f = \bar{u}$ is possible. For the $\pi^+\pi^+ \to \pi^+\pi^+$ scattering reaction one has $a = b = u$, $c = f = d$ or $a = b = \bar{d}$, $c = f = \bar{u}$. As before, this diagram contributes twice for both reactions as well. Note that because the two final state particles are the same, for the latter reaction the symmetrized diagram B_{2S} counts for the forward direction considered here too. Finally, we consider the third diagram B_3. This one shows up

only if the projection of the isospin changes. For the $\pi^+\pi^0 \to \pi^+\pi^0$ reaction we have $a = u$, $b = c = f = d$ or $a = \bar{d}$, $b = c = f = \bar{u}$, and therefore it contributes twice like the other two diagrams. Its symmetrized version corresponds to backward scattering as in the case of the first diagram, hence does not enter our calculations here.

Diagrams B_1, B_2, B_{2S} and B_3 are convolution integrals of the intermediate quark propagators, involved in the corresponding boxes, with the wave functions $\Psi_{ab}(k, P)$. Formulas for calculating each of them are provided in the Appendix. We can condensate all the book keeping described above in three equations defining the different charge scattering amplitudes in terms of B_1, B_2, B_{2S} and B_3:

$$\begin{aligned}
\langle\pi^+\pi^+|\mathcal{M}|\pi^+\pi^+\rangle &= 2(B_2 + B_{2S})\,,\\
\langle\pi^+\pi^-|\mathcal{M}|\pi^+\pi^-\rangle &= 2B_1\,,\\
\langle\pi^+\pi^0|\mathcal{M}|\pi^+\pi^0\rangle &= 2\frac{1}{2}(B_1 + B_2 + B_3)\,.
\end{aligned} \tag{3}$$

In these last equations we choose not to include in B_1, B_2, B_{2S} and B_3 the normalization factor $\frac{1}{\sqrt{2}}$ of the π_0 meson wave function. It originates the factor $\frac{1}{2}$ in the last equality. In the Appendix we show that $B_1 = B_3$, which is in part due to the proportionality between the different pion wavefunctions in equations (2).

In order to compute the isospin amplitudes we relate the meson–meson scattering amplitudes and the isospin amplitudes $\mathcal{M}_I$ ($I = 2, 1, 0$ labels total isospin), by means of isospin coupling coefficients. We obtain:

$$\begin{aligned}
\langle\pi^\pm\pi^\pm|\mathcal{M}|\pi^\pm\pi^\pm\rangle &= \mathcal{M}_2\,,\\
\langle\pi^\pm\pi^\mp|\mathcal{M}|\pi^\pm\pi^\mp\rangle &= \frac{1}{6}\mathcal{M}_2 + \frac{1}{2}\mathcal{M}_1 + \frac{1}{3}\mathcal{M}_0\,,\\
\langle\pi^\pm\pi^0|\mathcal{M}|\pi^\pm\pi^0\rangle &= \frac{1}{2}\mathcal{M}_2 + \frac{1}{2}\mathcal{M}_1\,,\\
\langle\pi^\pm\pi^\mp|\mathcal{M}|\pi^0\pi^0\rangle &= \frac{1}{3}\mathcal{M}_2 - \frac{1}{3}\mathcal{M}_0\,,\\
\langle\pi^0\pi^0|\mathcal{M}|\pi^0\pi^0\rangle &= \frac{2}{3}\mathcal{M}_2 + \frac{1}{3}\mathcal{M}_0\,.
\end{aligned} \tag{4}$$

By inverting the three first equations of this set of equations, we determine the amplitudes $\mathcal{M}_I$ in terms of the different charge scattering processes. Finally, by substituting the result back and using Eqs. (2), we get for $\mathcal{M}_I$

$$\begin{aligned}
\mathcal{M}_0 &= 3B_1 - B_2 + 2B_{2S} - 3B_3 = 2B_{2S} - B_2\,,\\
\mathcal{M}_1 &= 2(B_1 + B_3 - B_{2S}) = 2(2B_1 - B_{2S})\,,\\
\mathcal{M}_2 &= 2(B_2 + B_{2S})\,.
\end{aligned} \tag{5}$$

The amplitudes $\mathcal{M}_0$ and $\mathcal{M}_1$ are associated respectively with the contribution to meson–meson scattering of the exchange of the (isoscalar) σ and the (isovector) ρ mesons.

2.2. Adding gluon exchange to the model

In this section we consider gluon exchange between the quarks, which provides another mechanism for the effective meson–meson interaction.

The leading order diagrams that contribute are represented in the Figs. 4, 5 and 6. Gluon exchange on these diagrams are represented by the boxes with the label a G. These boxes are the sum of all the ladder diagrams.

We label the diagrams of Figs. 4, 5 and 6 respectively by B_{21}, B_{22} and B_{2S1}. Explicit formulas for them are given in the Appendix, by Eqs. (A.12), (A.15) and (A.18), respectively. They correspond to corrections of gluon-exchange to the quark-exchange.

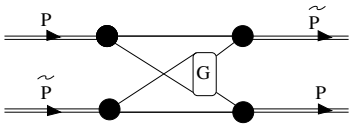

Fig. 4. Dressing up the crossed box: first contribution. Both quarks and gluons are exchanged.

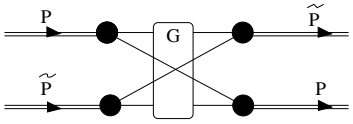

Fig. 5. Dressing up the crossed box: second contribution. Both quarks and gluons are exchanged.

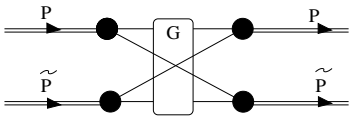

Fig. 6. Dressing up the symmetrized crossed box: first contribution. Other contributions are negligible. Both quarks and gluons are exchanged as well.

The diagrams in Fig. 7 (forward scattering) and Fig. 8 (backward scattering) are, in contrast, pure gluon exchange contributions to meson–meson scattering, which we label by B_{gf} and B_{gb}. They are only next to the leading order in $1/N_c$. The analytical formulas for their contribution is given in the Appendix, by Eqs. (A.24) and (A.25), respectively. The backward scattering diagram contributes only when the two pions in the final state have the same charge.

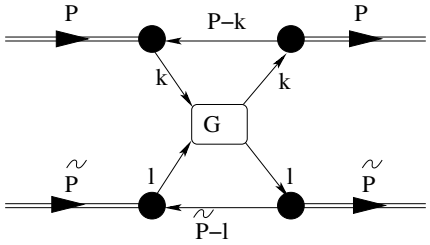

Fig. 7. Gluon exchange for forward scattering.

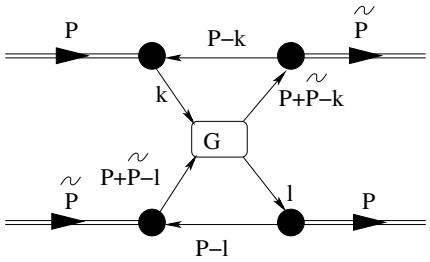

Fig. 8. Gluon exchange for backward scattering.

Including gluon exchange modifies Eq. (2) into

$$\begin{aligned}
\langle\pi^+\pi^+|\mathcal{M}|\pi^+\pi^+\rangle &= 2(\tilde{B}_2+\tilde{B}_{2S}+B_{gf}+B_{gb})\,,\\
\langle\pi^+\pi^-|\mathcal{M}|\pi^+\pi^-\rangle &= 2(\tilde{B}_1+B_{gf})\,,\\
\langle\pi^+\pi^0|\mathcal{M}|\pi^+\pi^0\rangle &= \tilde{B}_1+\tilde{B}_2+\tilde{B}_3+B_{gf}
\end{aligned} \tag{6}$$

with

$$\begin{aligned}
\tilde{B}_1 &\approx B_1\,,\\
\tilde{B}_3 &\approx B_1\,,\\
\tilde{B}_2 &= B_2+B_{21}+B_{22}\,,\\
\tilde{B}_{2S} &= B_{2S}+B_{2S1}\,.
\end{aligned} \tag{7}$$

Since the gluon corrections to the diagrams B_1 and B_3 are negligible, it is a good approximation to consider the equality between $\tilde{B}_1$ and $\tilde{B}_3$.

Due to these corrections, the amplitudes $\mathcal{M}_I$ in Eqs. (4) are also modified as follows:

$$\begin{aligned}
\mathcal{M}_0 &= 2\tilde{B}_{2S}-\tilde{B}_2+5B_{gf}\,,\\
\mathcal{M}_1 &= 2(2\tilde{B}_1-\tilde{B}_{2S}-B_{gb})\,,\\
\mathcal{M}_2 &= 2(\tilde{B}_2+\tilde{B}_{2S}+B_{gf}+B_{gb})\,.
\end{aligned} \tag{8}$$

3. Results

We considered different Bethe–Salpeter bound state wave functions calculated by the techniques introduced in [1] and [5]. The models built here differ from the ones studied in [1] in the value of the bare quark mass ratio, taken in that reference to be $m_{01}/m_{02} = 3/4$, but in this paper the ratio we considered to be unity. We took the pion mass value $m_\pi = 140\,\mathrm{MeV}$, as in [1]. The models are defined in the following way: for a given bare quark mass value we adjusted the coupling in such a manner that the pion mass comes out to be $m_\pi = 140\,\mathrm{MeV}$. The bare quark masses and the coupling uniquely define the model.

We collect the results for the masses and widths of the two mesonic isoscalar and isovector resonances obtained with these different models in Table I.

TABLE I

Values obtained for the masses of the σ-like and ρ-like resonances (m_σ and m_ρ) and their widths (Γ_σ and Γ_ρ), as a function of the quark–gluon coupling strength (g) and bare quark mass (m_0), all in MeV. The table also includes the values obtained for the dressed-quark masses.

Model	g	m_0	m	m_σ	Γ_σ	m_ρ	Γ_ρ
I	27.6	65.0	63.1	281	30	309	26
II	51.0	60.0	52.7	296	72	306	36
III	75.8	55.0	34.6	318	26	304	42
IV	91.4	52.0	6.70	337	35	295	27

Since Model II is the only model that satisfied the two conditions valid for the observed and physical σ and ρ resonances, $m_\rho > m_\sigma$ and $\Gamma_\rho < \Gamma_\sigma$, we single out Model II, out of the four seen to provide a realistic pion mass value, and show the features of its corresponding meson–meson resonances. Therefore, for the second set of parameters from Table I, we show in Fig. 9 the ground state quark–antiquark wave function, and subsequently, in Fig. 10 and in Fig. 11, we plot the scattering amplitudes $\mathcal{M}$.

The 't Hooft model has the feature of generating dressed quark masses smaller than the bare masses, and this effect increases with increasing magnitude of the coupling. As a consequence, the mass of the σ-like resonance gets closer to the threshold with decreasing quark–gluon coupling. Nevertheless, the mass of the ρ-like resonance is getting further away from the threshold as the coupling decreases. This is indicative that the ρ-like resonance has a structure more complex than two pion clusters. That the σ-like mass resonance decreases, while the ρ-like mass resonance increases for decreasing

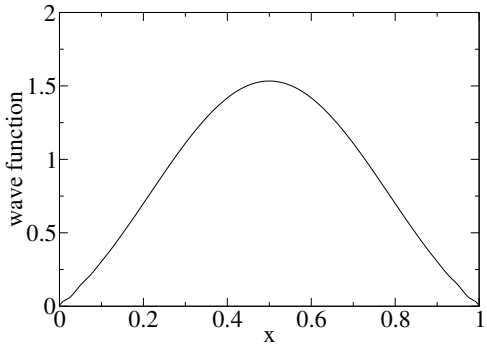

Fig. 9. The ground state wave function for Model II on Table I.

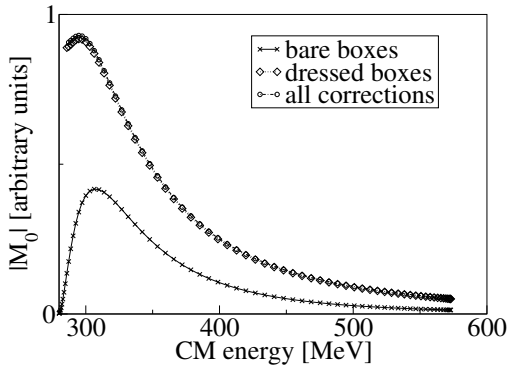

Fig. 10. The $\mathcal{M}$ amplitudes for the σ meson in case II on Table I. The bare term and the respective corrections are shown separately. The pure gluon exchange is negligible.

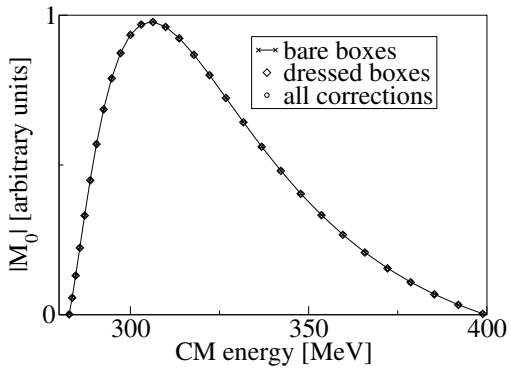

Fig. 11. The $\mathcal{M}$ amplitudes for the ρ meson in case II on Table I. The bare term and the dressed term are shown separately. All corrections are negligible.

quark–gluon coupling, is behind the success of Model II (with the intermediate value for that coupling) in providing $m_\rho > m_\sigma$ and $\Gamma_\rho < \Gamma_\sigma$ of the real resonances. The running values of the quark–gluon coupling show that these inequalities arise within the 't Hooft model when the quark–antiquark state, *i.e.* the pion, is weakly bound or shallow, but not as shallow as in Model I.

Comparing Figs. 10 and 11, respectively, for the isospin zero and isospin 1 components of the meson–meson amplitude, we conclude that for the sigma-like exchange (isospin 0 case), the dressing of the boxes due to gluon exchange dominates the other "pure" gluon-exchange corrections. For the case of the ρ-like meson exchange, however, all contributions involving gluons are seen to be negligible. This is consistent with a picture for the σ resonance where the gluon degrees of freedom are very much present, essentially through the dressing of the quark-exchange boxes.

We have also investigated the chiral limit (where the bare quark mass m_0 vanishes) of the meson–meson scattering amplitudes. We found that all amplitudes vanish in that limit, even without including gluon exchange between mesons. This is in contrast with the findings of [3], where those diagrams were essential for a correct behavior in the chiral limit. This difference is due not only to the reduced dimensionality in our framework, but also to the use here of the Minkowski metric instead of the Euclidean metric.

4. Conclusions and discussion

We have included isospin in the 't Hooft model, which is an *ab initio* QCD in $1 + 1$ dimensions, and calculated meson–meson scattering. The results show that the 't Hooft model can accommodate the description of meson–meson scattering in terms of exchanges of isoscalar (σ-like) and and isovector (ρ-like) mesons, which has been for a long time the picture suggested by experiment, and was recently verified by phenomenological theories [2] for confinement.

We verified that gluon exchange helps differentiating the two different isospin resonances present in the meson–meson scattering amplitude. Specifically, gluon exchanges affect dramatically the isoscalar σ-like resonance. We found also that all gluon exchange corrections vanish for the chiral limit to be satisfied.

Research supported by the Fundação para a Ciência e Tecnologia, Portugal, under grant contract number SFRH/BPD/5661/2001. We thank Jiri Adam for useful discussions.

Appendix A

To give a flavor how do we get the definition of the amplitudes, let us concentrate first on the first amplitude. By drawing down the non-symmetrized version of the first diagram, one gets:

$$B_1 = \frac{1}{N_c}\int_{-\infty}^{\infty} dk_- \int_{-\infty}^{\infty} dk_+ \Psi(-k,-P)\Psi(k,\tilde{P})\Psi(P+\tilde{P}-k,P)\Psi(k-P-\tilde{P},-\tilde{P}) \times S(k)S(k-\tilde{P})S(k-P-\tilde{P})S(k-P)\,, \tag{A.1}$$

where S is the quark propagator as given in [1]. For the quark that has the momentum k, this propagator is

$$S(k) = \frac{k_-}{2k_-k_+ - m^2 + i\varepsilon}\,. \tag{A.2}$$

Simplifying by k_- one gets

$$S(k) = \frac{1}{k_+ - k_1}\,, \tag{A.3}$$

where k_1 is defined by Eq. (A.5). Similarly all other propagators are reduced to similar entities. and that is how we arrive to the following equations defining B_1, B_2, B_{2S} and B_3:

$$N_c B_1 = \int_{-\infty}^{\infty} dk_- \int_{-\infty}^{\infty} dk_+ \Psi(-k,-P)\Psi(k,\tilde{P})\Psi(P+\tilde{P}-k,P)\Psi(k-P-\tilde{P},-\tilde{P}) \times \frac{1}{k_+-k_1}\frac{1}{k_+-k_2}\frac{1}{k_+-k_3}\frac{1}{k_+-k_4}\,,$$

$$N_c B_2 = \int_{-\infty}^{\infty} dk_- \int_{-\infty}^{\infty} dk_+ \Psi(-k,-P)\Psi(k,\tilde{P})\Psi(P-k,P)\Psi(-k,-\tilde{P}) \times \frac{1}{(k_+-k_1)^2}\frac{1}{k_+-k_2}\frac{1}{k_+-k_4}\,,$$

$$N_c B_{2S} = \int_{-\infty}^{\infty} dk_- \int_{-\infty}^{\infty} dk_+ \Psi(k,P)\Psi(-k,-P)\Psi(k-P-\tilde{P},-\tilde{P})\Psi(P+\tilde{P}-k,\tilde{P}) \times \frac{1}{(k_+-k_4)^2}\frac{1}{k_+-k_1}\frac{1}{k_+-k_3'},$$

$$N_{\rm c}B_3 = \int\limits_{-\infty}^{\infty} dk_- \int\limits_{-\infty}^{\infty} dk_+ \Psi(-k,-P)\Psi(k,\tilde{P})\Psi(P+\tilde{P}-k,P)\Psi(k-P-\tilde{P},-\tilde{P}) \times \frac{1}{k_+ - k_1}\frac{1}{k_+ - k_2}\frac{1}{k_+ - k_3}\frac{1}{k_+ - k_4}\,. \tag{A.4}$$

The poles of the propagators are defined as

$$\begin{aligned} k_1 &= \frac{m_1^2}{2k_-} - i\varepsilon\,\mathrm{sign}(k_-)\,, \\ k_2 &= \tilde{P}_+ + \frac{m_2^2}{2(k_- - \tilde{P}_-)} - i\varepsilon\,\mathrm{sign}(k_- - \tilde{P}_-)\,, \\ k_3 &= P_+ + \tilde{P}_+ + \frac{m_1^2}{2(k_- - P_- - \tilde{P}_-)} - i\varepsilon\,\mathrm{sign}(k_- - P_- - \tilde{P}_-)\,, \\ k_3' &= P_+ - \tilde{P}_+ + \frac{m_1^2}{2(k_- - P_- + \tilde{P}_-)} - i\varepsilon\,\mathrm{sign}(k_- - P_- + \tilde{P}_-)\,, \\ k_4 &= P_+ + \frac{m_2^2}{2(k_- - P_-)} - i\varepsilon\,\mathrm{sign}(k_- - P_-) \end{aligned} \tag{A.5}$$

and the light cone components of the momenta in the usual fashion:

$$\begin{aligned} k_+ &= \frac{1}{\sqrt{2}}(k^0 + k^1)\,, \\ k_- &= \frac{1}{\sqrt{2}}(k^0 - k^1)\,. \end{aligned} \tag{A.6}$$

We can see that the definitions of B_1 and B_3 are the same, therefore $B_1 = B_3$.

We first describe how B_1 is calculated. In order to perform the k_+ integration, one needs to close the contour in the complex plane and consider the residues of all poles inside the contour. There are 16 different possible combinations of signs of the imaginary parts of the poles. Some of these cases can be excluded, because they correspond to values of k_- which make the k_+ integral vanish.

For instance, a pole k_1 in the upper half plane implies that the pole k_2 cannot be in the lower half-plane, otherwise one would have $k_- > \tilde{P}_- = (\sqrt{\mu^2+p^2}+p)/\sqrt{2} > 0,$ in contradiction with the initial hypothesis $k_- < 0$. Likewise the poles k_3 and k_4 cannot be in the lower half-plane either. Therefore, if k_1 is in the upper half-plane, the other 3 poles are also in the upper half plane. This would imply the k_+ integral to vanish, since one may close the contour below the k_+ axis. Therefore, we can exclude the case when k_1 is in the upper half plane.

After a detailed analysis one finds that there are only three cases that have a non-vanishing contribution to the integral: *(i)* only k_3 is in the upper half plane, *(ii)* the poles k_2 and k_3 are in the upper half plane, *(iii)* only k_1 is in the lower half plane.

As for case *(i)*, it implies $k_- > \tilde{P}_-$ and $k_- < P_- + \tilde{P}_-$. Under these circumstances, $\psi(P+\tilde{P}-k,P) = 2/(\pi i)(k_3-k_2)|_{\varepsilon=0}\varphi((P+\tilde{P}-k)_-/P_-)$ and $\psi(k-P-\tilde{P},-\tilde{P}) = 2/(\pi i)(k_2-k_1)|_{\varepsilon=0}\varphi((P+\tilde{P}-k)_-/\tilde{P}_-)$, where φ is the solution of the 't Hooft equation, while the other vertex functions have to be evaluated using

$$\Psi(p,r) = \frac{g^2}{-i\pi^2}\mathcal{P}\int dk_- D(k_-)\,\varphi(p_-+k_-,r_-)\,, \tag{A.7}$$

as done in [1]. D is the gluon propagator and g is the quark–gluon coupling strength. The contribution from case *(i)* becomes

$$\begin{aligned} B_{1(i)} \;=\; & -\frac{2i}{\pi^3 N_{\rm c}} \int\limits_{\tilde{P}_-}^{\tilde{P}_-+P_-} dk_- \frac{1}{(k_3-k_4)} \\ & \times\varphi\left(\frac{(P+\tilde{P}-k)_-}{P_-}\right)\varphi\left(\frac{(P+\tilde{P}-k)_-}{\tilde{P}_-}\right)\Psi(-k,-P)\Psi(k,\tilde{P})\,. \end{aligned} \tag{A.8}$$

After treating the other two cases in a similar fashion, we find that B_1 is:

$$\begin{aligned} B_1 \;=\; & -\frac{2i}{\pi^3 N_{\rm c}} \int\limits_{\tilde{P}_-}^{\tilde{P}_-+P_-} dk_- \frac{1}{(k_3-k_4)} \\ & \times\varphi\left(\frac{(P+\tilde{P}-k)_-}{P_-}\right)\varphi\left(\frac{(P+\tilde{P}-k)_-}{\tilde{P}_-}\right)\psi(-k,-P)\psi(k,\tilde{P}) \\ & +\frac{2i}{\pi^3 N_{\rm c}} \int\limits_{0}^{P_-} dk_- \frac{1}{(k_1-k_3)} \\ & \times\left(\varphi\left(\frac{k_-}{P_-}\right)\right)^2 \Psi(k_- - P_- - \tilde{P}_-,-\tilde{P})\Psi(P_- + \tilde{P}_- - k_-,P) \\ & -\frac{2i}{\pi^3 N_{\rm c}} \int\limits_{P_-}^{\tilde{P}_-} dk_- \left(\frac{k_3-k_4}{(k_2-k_3)(k_2-k_4)} + \frac{k_2-k_1}{(k_3-k_1)(k_3-k_2)}\right) \\ & \times\varphi\left(\frac{k_- - P_- - \tilde{P}_-}{-v\tilde{P}_-}\right)\varphi\left(\frac{k_-}{\tilde{P}_-}\right)\Psi(P_- + \tilde{P}_- - k_-,-P)\Psi(-k_-,-P). \end{aligned} \tag{A.9}$$

Likewise, we compute B_2 which we find to be

$$B_2 = \frac{2i}{\pi^3 N_{\rm c}} \int\limits_{P_-}^{\tilde{P}_-} dk_- \frac{1}{k_2 - k_4} \left(\varphi \left(\frac{k_-}{\tilde{P}_-} \right) \right)^2 \Psi(-k_-, -P) \Psi(k_-, P)$$

$$- \frac{i}{2\pi N_{\rm c}} \left(\frac{2}{\pi} \right)^4 \int\limits_0^{P_-} dk_- (2k_1 - k_2 - k_4) \left(\varphi \left(\frac{k_-}{\tilde{P}_-} \right) \right)^2 \left(\varphi \left(\frac{k_-}{P_-} \right) \right)^2 . \quad \text{(A.10)}$$

Similarly, B_{2S} is:

$$\begin{aligned} B_{2S} \quad &= - \frac{i}{2\pi N_{\rm c}} \left(\frac{2}{\pi} \right)^4 \int\limits_0^{P_-} dk_- (k_1 + k_3' - 2k_4) \\ &\times \left(\varphi \left(\frac{k_-}{P_-} \right) \right)^2 \left(\varphi \left(\frac{k_- - \tilde{P}_- + P_-}{P_-} \right) \right)^2 \\ &+ \frac{i}{2\pi N_{\rm c}} \left(\frac{2}{\pi} \right)^2 \int\limits_{P_- - \tilde{P}_-}^{0} dk_- \frac{1}{k_3 - k_1} \\ &\times \left(\varphi \left(\frac{k_- + \tilde{P}_- - P_-}{\tilde{P}_-} \right) \right)^2 \Psi(-k, -P) \Psi(k, P) . \end{aligned} \quad \text{(A.11)}$$

At the end we set $\varepsilon = 0$ and $m_1 = m_2$.

The terms involving both gluon and quark exchange are discussed as follows. the crossed box has two corrections, B_{21} and B_{22}. The first is approximated as:

$$B_{21} = \frac{4i}{\pi^6} \int\limits_0^{P_-} dk_- \int\limits_0^{\tilde{P}_-} dl_- \varphi \left(\frac{k_-}{P_-} \right) \varphi \left(\frac{k_-}{\tilde{P}_-} \right) \varphi \left(\frac{l_-}{P_-} \right) \varphi \left(\frac{l_-}{\tilde{P}_-} \right) G_{21} , \quad \text{(A.12)}$$

with

$$G_{21} = -g^2 \Sigma_n \frac{2}{\pi^3} \frac{\varphi_n \left(\frac{k_-}{(k_- + l_-)} \right) \varphi_n \left(\frac{l_-}{(k_- + l_-)} \right)}{M_n^2 - 2(k_2 + l_2)(k_- + l_-)} . \quad \text{(A.13)}$$

Here the index n refers to the order of the mesonic bound state (first eigenvalue, second, *etc.*), M_n φ_n to their bound state mass and wave function, g is the quark–gluon coupling strength, while k_2 and l_2 are

$$k_2 = P_+ + \frac{m^2}{2(k_- - P_-)} , \qquad l_2 = \tilde{P}_+ + \frac{m^2}{2(k_- - \tilde{P}_-)} . \quad \text{(A.14)}$$

The second is approximated as:

$$B_{22} = \frac{4i}{\pi^6} \int_0^{P_-} dk_- \int_0^{P_-} dl_- \varphi\left(\frac{k_-}{P_-}\right) \varphi\left(\frac{k_-}{\tilde{P}_-}\right) \varphi\left(\frac{l_-}{P_-}\right) \varphi\left(\frac{l_-}{\tilde{P}_-}\right) G_{22}\,, \quad \text{(A.15)}$$

with

$$G_{22} = g^2 \frac{2}{\pi^3} \sum_n \frac{\varphi_n\left(\frac{P_- - k_-}{P_- + \tilde{P}_- + l_- - 2k_-}\right) \varphi_n\left(\frac{\tilde{P}_- - k_-}{P_- + \tilde{P}_- + l_- - 2k_-}\right)}{M_n^2 - 2(P_+ + \tilde{P}_+ + l_1 - 2k_1)(P_- + \tilde{P}_- + l_- - 2k_-)}\,, \quad \text{(A.16)}$$

where the momenta k_2 and l_2 are

$$k_2 = P_+ + \frac{m^2}{2(k_- - P_-)}\,, \qquad l_2 = \tilde{P}_+ + \frac{m^2}{2(k_- - \tilde{P}_-)}. \quad \text{(A.17)}$$

The third is approximated as:

$$B_{2S1} = \frac{4i}{\pi^6} \int_0^{P_-} dk_- \int_0^{P_-} dl_- \varphi\left(\frac{k_-}{P_-}\right)^2 \varphi\left(\frac{\tilde{P}_- - P_- - l_-}{\tilde{P}_-}\right)^2 G_{2S1}\,, \quad \text{(A.18)}$$

with

$$G_{2S1} = g^2 \frac{2}{\pi^3} \sum_n \frac{\varphi_n^2\left(\frac{\tilde{P}_- - k_-}{2P_- - k_- - l_-}\right)}{M_n^2 - 2(2P_+ - k_2 - l_2)(2P_- - k_- - l_-)}\,, \quad \text{(A.19)}$$

where the momenta k_2 and l_2 are

$$k_2 = P_+ + \frac{m^2}{2(k_- - P_-)}\,, \qquad l_2 = P_+ + \frac{m^2}{2(l_- - P_-)}\,. \quad \text{(A.20)}$$

We now discuss the gluon exchange terms.

For the backward scattering term, first we define the terms A_1 and A_2:

$$\begin{aligned} A_1 &= \frac{1}{\pi^2(k_3 - k_1)} \varphi\left(\frac{k_- - P_-}{\tilde{P}_-}\right) \Psi(k, -P)\theta(k_- - P_-)\theta(P_- + \tilde{P}_- - k_-) \\ &\quad - \frac{1}{\pi^2(k_1 - k_3)(k_1 - k_2)} \Psi(k - P, -P)\theta(P_- - k_-)\Psi(P - k, \tilde{P}) \\ A_2 &= \frac{1}{\pi(l_3 - l_1)} \varphi\left(\frac{l_- - P_-}{\tilde{P}_-}\right) \Psi(l, -P)\theta(l_- - P_-)\theta(P_- + \tilde{P}_- - l_-) \\ &\quad - \frac{1}{\pi^2(l_1 - l_3)(l_1 - l_2)} \Psi(l - P, -P)\Psi(P - l, \tilde{P})\theta(P_- - l_-)\,, \end{aligned} \quad \text{(A.21)}$$

where the momenta k_1, k_2, k_3, l_1, l_2 and l_3 are

$$\begin{aligned} k_1 &= \frac{m^2}{2k_-}\,, \\ k_2 &= P_+ + \frac{m^2}{2(k_- - P_-)}\,, \\ k_3 &= \tilde{P}_+ + P_+ + \frac{m^2}{2(k_- - \tilde{P}_- - P_-)}\,, \\ l_1 &= \frac{m^2}{2l_-}\,, \\ l_2 &= P_+ + \frac{m^2}{2(l_- - P_-)}\,, \\ l_3 &= \tilde{P}_+ + P_+ + \frac{m^2}{2(l_- - \tilde{P}_- - P_-)}\,. \end{aligned} \tag{A.22}$$

We also give the explicit form of G, the dressed two quark propagator

$$G_{gb} = \sum_n \frac{\varphi_n\left(\frac{k_-}{k_- + P_- + \tilde{P}_- + l_-}\right)\varphi_n\left(\frac{P_- + \tilde{P}_- k_-}{P_- + \tilde{P}_- - k_- + l_-}\right)}{M_n^2 - 2(k_1 + l_3)(k_- + P_- + \tilde{P}_- + l_-)}\,. \tag{A.23}$$

By neglecting the contribution of the pole of G, we have

$$B_{gb} = g^2 \frac{8i}{\pi^3 N_c^2} \int_0^{P_- + \tilde{P}_-} dk_- \int_0^{P_- + \tilde{P}_-} dl_- A_1 A_2 G_{gb}\,. \tag{A.24}$$

The forward scattering term is much simpler:

$$B_{gf} = -\frac{8i}{\pi^3 N_c^2} \int_0^{P_- + \tilde{P}_-} dk_- \int_0^{P_- + \tilde{P}_-} dl_- \left(\varphi\left(\frac{k_-}{P_-}\right)\varphi\left(\frac{l_-}{\tilde{P}_-}\right)\right)^2 G_{gf}\,, \tag{A.25}$$

where the propagator G is also simpler

$$G_{gf} = g^2 \sum_n \frac{\varphi_n^2\left(\frac{k_-}{k_- + l_-}\right)}{M_n^2 - 2(k_1 + l_2)(k_- + l_-)}\,, \tag{A.26}$$

and the notations for k_1 and l_2 are modified as

$$k_1 = P_+ + \frac{m^2}{2(k_- - P_-)}\,, \qquad l_2 = \tilde{P}_+ + \frac{m^2}{2(k_- - \tilde{P}_-)}\,. \tag{A.27}$$

REFERENCES

[1] Z. Batiz, M.T. Peña, A. Stadler, *Phys. Rev.* **C69**, 035209 (2004).

[2] S.R. Cotanch, P. Maris, *Phys. Rev.* **D66**, 116010 (2002).

[3] P. Bicudo, S. Cotanch, F. Llanes-Estrada, P. Maris, E. Ribeiro, A. Szczepaniak, *Phys. Rev.* **D65**, 076008 (2002).

[4] D.V. Bugg, *Phys. Lett.* **B572**, 1 (2003).

[5] Z. Batiz, F. Gross, *Phys. Rev.* **D69**, 074006 (2004).